CONF-960238--8

LA-UR- 95-3947

Title: Damage Identification Algorithms Applied to Numerical MOdal Data from a Bridge

Author(s): David V. Jauregui, LANL, ESA-EA
Charles R. Farrar, LANL, ESA-EA

Submitted to: 14th International Modal Analysis Conference
Dearborn, Michigan
February 12-15, 1996

MASTER

Los Alamos
NATIONAL LABORATORY

DAMAGE IDENTIFICATION ALGORITHMS APPLIED TO NUMERICAL MODAL DATA FROM A BRIDGE

David V. Jauregui and Charles R. Farrar

Engineering Analysis Group (ESA-EA)
MS P946
Los Alamos National Laboratory
Los Alamos, NM 87545

ABSTRACT. This paper extends the work summarized in the accompanying paper "Comparison of Damage Identification Algorithms on Experimental Modal Data From A Bridge." A finite element model of the continuous three-span portion of the I-40 bridges, which once crossed the Rio Grande in Albuquerque, NM, was constructed. Following the experimental modal analysis, the bridge tests are repeated analytically using benchmarked finite element models of the bridge. A combination of shell and beam elements form the bridge model. Damage was simulated by creating adjacent nodes and disconnecting the elements on either side of the crack. However, because of the discretization of the finite element models only the final three levels of damage were evaluated. In addition to the analytical simulation of the experiments, the girder crack was repositioned at other potential damage locations. Analytical modal parameters were extracted through signal processing techniques, similar to those used in the experimental investigation and subsequently fed into damage identification routines. These routines have been adapted from those presented at past IMAC conferences and are identical to the ones used in the experimental investigation reported in the accompanying paper. This study provides a direct comparison of the relative accuracy of these different damage identification methods when they are applied to a set of standard numerical problems. The numerical models allow a variety of damage scenarios to be studied once the models have been benchmarked against experimental data.

1. INTRODUCTION.

Because the Interstate 40 (I-40) bridges over the Rio Grande in Albuquerque, New Mexico were to be razed during the summer of 1993, investigators from New Mexico State University (NMSU) were able to introduce simulated cracks into the structure in order to test various damage identification methods. To support this research effort, Los Alamos National Laboratory (LANL) performed experimental modal analyses [1, 2], and developed experimentally verified numerical models of the bridge [3].

In this paper five damage identification methods that have been reported in the technical literature were applied numerically generated modal data obtained from the finite element models of the I-40 bridge. Once benchmarked against experimental data, these numerical models allow a variety of damage scenarios to be investigated. In addition to simulating the experimental damage cases, these models were used to examine damage closer to a support location and a case where damage was inflicted at two locations.

These damage identification methods and the geometry of the I-40 bridge are briefly discussed in an accompanying paper [4]. A more detailed summary of the damage identification methods can be found in the cited references for each method. These methods are referred to as: 1.) the damage index method [5], 2.) the mode shape curvature method [6], 3.) the change in flexibility method [7], 4.) the change in uniform flexibility curvature method [8], and 5.) the change in stiffness method [9]. All these methods require mode shape amplitudes before and after damage. For methods 3, 4, and 5, the mode shapes must be unit-mass normalized. Methods 3, 4, and 5 also require resonant frequencies measured before and after damage. For a more detailed summary of the application of these damage identification methods to the I-40 Bridge data, both numerical and experimental, the reader is referred to [10].

Damage or fault detection, as determined by changes in the dynamic properties or response of structures, is a subject which has received considerable attention in the technical literature beginning approximately 30 years ago. A significant increase in reported studies has appeared during the last five years. The basic idea is that modal parameters, notably frequencies, mode shapes, and modal damping, are a function of the physical properties of the structure

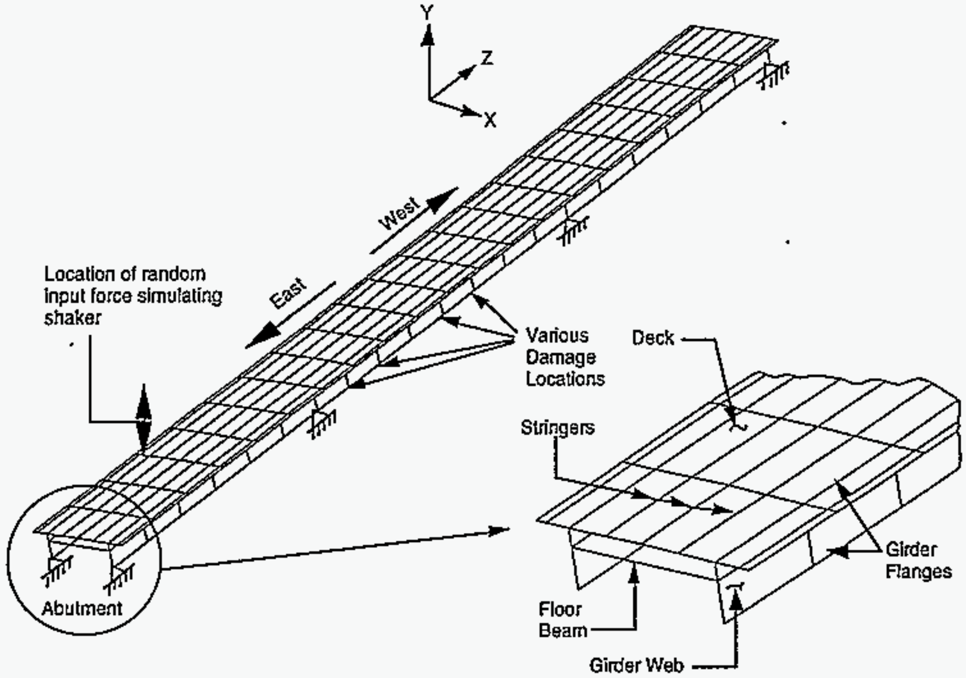

Fig. 1 Finite element model of the I-40 bridge.

(mass, damping, stiffness, and boundary conditions). Therefore, changes in physical properties of the structure, such as its stiffness or flexibility, will cause changes in the modal properties. Early methods for detecting damage based on changes in the structure's dynamic properties primarily examined changes in the resonant frequencies. However, this parameter has proved to be insensitive to lower levels of damage and does not provide a means to locate the damage. Current methods that have shown promise in both detecting damage at an early stage and locating the damage examine changes in the mode shapes of the structure. A detailed summary of damage identification from changes in dynamic properties of structures will be given in [11].

In choosing the damage identification methods to be compared, the authors have limited their study to those requiring only measured responses before and after damage as opposed to those requiring a correlatd finite element model. Although the statement will be made that the finite element models in this study were benchmarked against measured modal data, this benchmarking was done only to verify that the models are accurately preciting the dynamic respons of the structure. The authors acknowledge that many other damage identification methods exist and an obvious extension of this work would be to apply these methods to the same data sets reported herein and in the accompanying paper.

2. FINITE ELEMENT MODELS

Using benchmarked finite element models as described in [3], forced vibration tests similar to the ones conducted on the I-40 Bridge were simulated numerically. All dynamic analyse were performed with the commercial finite element code on a CRAY Y-MP computer. Results of the analyses were post-processed using finite element code's post-processing routine, also on the CRAY. Mesh generation was done with commercial pre-processor on a workstation.

2.1 MODEL GEOMETRY AND BOUNDARY CONDITIONS

The finite element model of the bridge superstructure, Fig. 1, included a total of 1235 nodes and 548 elements. With this mesh configuration the bridge model had 7032 degrees of freedom. Eight-node shell elements were chosen to model the web of the two girders and the bridge deck whereas three-node beam elements were used to model the girder flanges, the floor beams, and the stringers. Detailing of the bridge model at the abutment end is also shown on Fig. 1. Horizontal and vertical stiffeners on the plate girder, the diagonal bracing, and the concrete reinforcement were not included in this model. Previous studies [3], where the individual stiffeners were modeled (35,160 DOF model), showed no significant variation in the global dynamic properties from the model used in this study.

Boundary conditions are enforced at the support locations shown on Fig. 1 where the bridge is supported by the concrete piers. Note that when defining the boundary conditions, no attempt was made to model the piers. Instead, at all support locations, translation in the three global directions X, Y, and Z is constrained. Although the piers must be modeled to accurately simulate the dynamic response of the I-40 Bridge, for the purpose of comparing different damage identification methods they can be neglected thus reducing the required computational time. To further simulate the actual constraints on the base of the plate girders at the piers, the out-of-plane rotations (about the Y and Z axes shown in Fig. 1) are also constrained at these locations.

2.2 MATERIAL PROPERTIES

Generic material properties for steel were specified as

E_{steel} = 29,000,000 psi (200 GPa),
ν_{steel} = 0.3, and
μ_{steel} = 0.284 lbm / in^3 (786 kg/m^3).

Generic concrete properties were specified as

$E_{concrete}$ = 3,600,000 psi (24.8 GPa),
$\nu_{concrete}$ = 0.2, and
$\mu_{concrete}$ = 145 lbm / ft^3 (232 kg/m^3).

2.3 SIMULATION OF DAMAGE

As shown in Fig. 2, three levels of damage similar to the final three girder cuts imposed during the I-40 Bridge tests were simulated by creating additional nodes at the vicinity of the crack and redefining the finite element discretization of the plate girder web and bottom flange in this region.

(a)

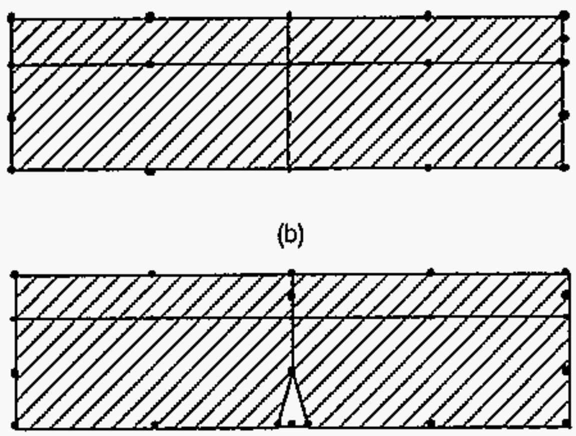

(b)

Fig. 2 Finite element modeling of the main girder (a) before damage and (b) after damage.

The second level of damage was simulated by disconnecting the shell elements representing the lower one-third of the web and allowing the bottom flange to remain connected using a new beam element. For the third phase of damage, the new beam element directly below the termination of the web cut are altered to one-half their original cross-sectional area. Finally, the new bottom flange element connecting the two damaged portions of the girder is removed to simulate the final damage condition. This method of modeling the damage changes the geometry only, and does not introduce nonlinearities into the model. Therefore, a linear modal analysis can be performed to ascertain the effects of this damage on the dynamic properties of the structure. A summary of the simulated damage conditions at the bridge midspan is provided in Table I.

TABLE I

Summary of Damage Cases A-1 through A-8

Damage Case	Location of Damage on Middle Span of the North Girder	Damage Description
A-1	midspan	lower one-third portion of web cut
A-2	midspan	lower one-third portion of web plus half of bottom flange cut
A-3	midspan	lower one-third portion of web plus entire bottom flange cut
A-4	one location: halfway between midspan and east support	lower one-third portion of web plus entire bottom flange cut
A-5	one location: one floor-beam-panel away from east support	lower one-third portion of web plus entire bottom flange cut
A-6	two locations: halfway between midspan and east support; one floor-beam-panel west of midspan	lower one-third portion of web plus entire bottom flange cut
A-7	one location: halfway between midspan and east support	lower one-third portion of web cut
A-8	one location: one floor-beam-panel away from east support	lower one-third portion of web cut

In addition to the damage simulations at the girder midspan, other damage scenarios were modeled to evaluate the dynamic response of the bridge with damage at different locations. Five damage scenarios were modeled at different locations on the north girder in the central span. Damage cases A-4 through A-8 correspond to the additional five damage scenarios. A summary of the additional damage cases is also provided in Table I.

The final case (A-9) did not involve altering the finite element model. Instead, the original forcing function (discussed below) is replaced with a different force-time history that had an identical frequency content as the one used in the analyses of cases A-1 through A-8. Case A-9 was used to test that the damage identifications methods do not yield a "false positive" reading, that is, they do not identify damage when damage has not occurred.

2.4 LOADING

For the I-40 Bridge tests, a 2000 lb (8900 N) peak amplitude random excitation was applied by the a shaker. A random signal was generated to simulate the input force applied by the shaker during the actual experimental modal testing of the I-40 Bridge. The signal was specified so that it would have a uniform power spectral density in the range of 2 to 12 Hz and a peak amplitude of 2000 lbs (8900 N). The random signal was defined with 1024 pts at 0.025 s time intervals. Plots of the generated random signal along with its power spectral density are provided in Figs. 3 and 4, respectively. The duration of force-time history is 25.6 seconds and the

Nyquist frequency for the signal is 20 Hz. This generated random force is applied to the model as a time-varying concentrated vertical load at a nodal point that approximates the position of the shaker during the forced vibration tests. The random force was applied directly above the south girder at the midpoint of the east span as shown in Fig. 1.

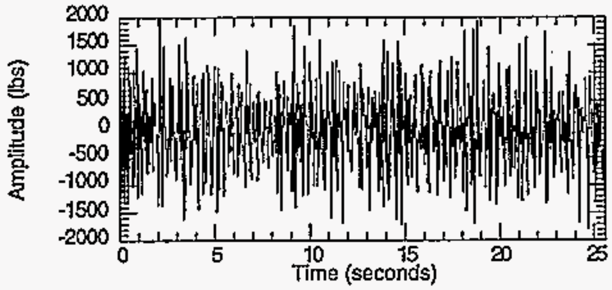

Fig. 3 Generated random signal used to simulate the input force applied by the shaker.

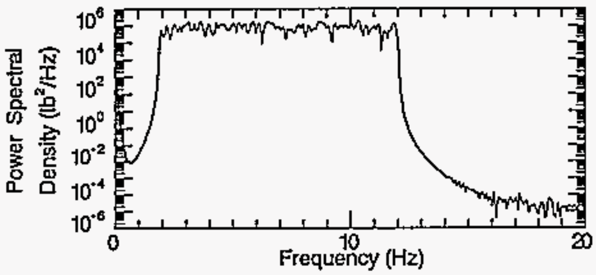

Fig. 4 Power spectral density of random input force in the frequency range of 0 - 20 Hz.

3. EIGENVALUE ANALYSIS

Before conducting the forced vibration dynamic analyses of the I-40 Bridge, eigenvalue analyses were performed in order to identify the resonant frequencies of the first three modes. This analysis was first conducted with the bridge in undamaged condition and then repeated for each state of damage (Cases A-1 through A-8) to determine the changes, if any, in the resonant frequencies that result from the damage.

Figure 5 shows the first bending mode identified from the eigenvalue analysis of the undamaged bridge. The same mode identified for damage case A-3 is shown in Fig. 6. When this level of damage is introduced, there is a decrease in the resonant frequency of the first mode (approximately 4.2%) along with a 0.78% reduction for the second mode frequency. No changes were detected in the third mode frequency after damage case A-3 was introduced. This response was expected because one of the nodes for the third mode coincided with the damage location. Table III summarize the changes in resonant frequencies for the first three modes that resulted from the various damage scenarios. Examination of this table shows that when reported to three significant figures, there is at most a 4.2% change in the resonant frequencies for the damage cases that were studied. No significant changes in the resonant frequencies were detected for the first torsional and second bending modes.

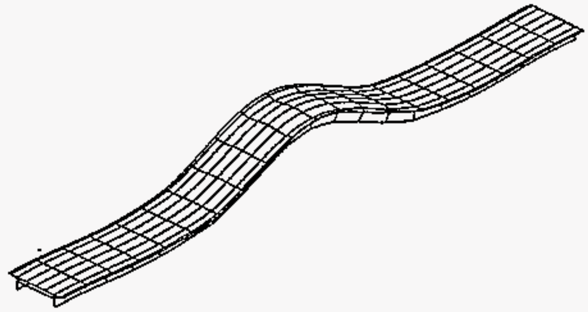

Fig. 5 First bending mode of the undamaged structure.

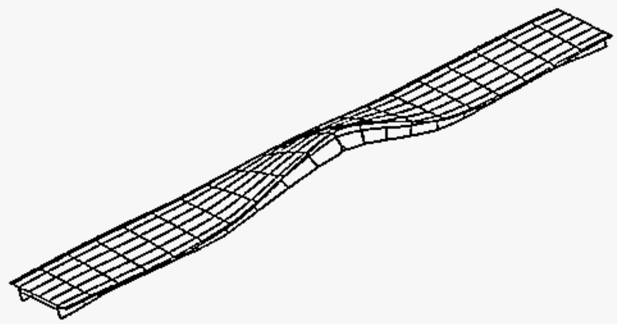

Fig. 6 First bending Mode corresponding to the damage condition A-3.

TABLE III

Resonant Frequencies Predicted By Finite Element Models of the Various Damage Scenarios

Damage Case	First Bending Mode Freq. (Hz)[1]	First Torsional Mode Freq. (Hz)[1]	Second Bending Mode Freq. (Hz)[1]
No Damage	3.79	3.87	5.09
A-1	3.79 (0.0%)	3.87 (0.0%)	5.09 (0.0%)
A-2	3.79 (0.0%)	3.87 (0.0%)	5.09 (0.0%)
A-3	3.63 (4.2%)	3.84 (0.8%)	5.09 (0.0%)
A-4	3.79 (0.0%)	3.87 (0.0%)	5.07 (0.4%)
A-5	3.63 (4.2%)	3.85 (0.5%)	5.07 (0.4%)
A-6	3.69 (2.6%)	3.85 (0.5%)	5.07 (0.4%)
A-7	3.79 (0.0%)	3.87 (0.0%)	5.09 (0.0%)
A-8	3.79 (0.0%)	3.87 (0.0%)	5.09 (0.0%)

[1]Values in parentheses are the percent change from the undamaged case

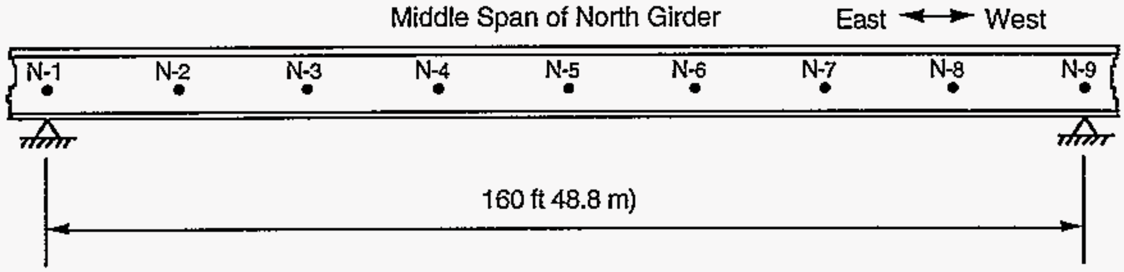

Fig. 7 Simulated measurement locations.

4. TIME-HISTORY ANALYSES

Using the random force input shown in Fig. 3, a dynamic time history analysis was conducted using modal superposition and the responses (i.e., vertical acceleration-time histories) at the nine monitored nodal points were recorded. The discretization used in the finite element model did not have node points corresponding to the actual refined set of 11 discrete measurement locations discussed in [4]. Instead, nine equally spaced nodal point accelerations were monitored. The nine nodes are spaced longitudinally at equal distances of roughly 20 ft. (6.10 m), which are locations where the floor beams frame into the main girder. In the vertical direction, the monitored nodes are located approximately one-third the girder height above the bottom flange. The nine response locations are shown in Fig. 7. A typical response at location N-5 is shown in Figs. 8. When implementing this analysis method, it is assumed that the structure is linear and that a sufficient number of modes have been extracted to accurately model the structure's dynamic response. The first ten modes were used in this analysis.

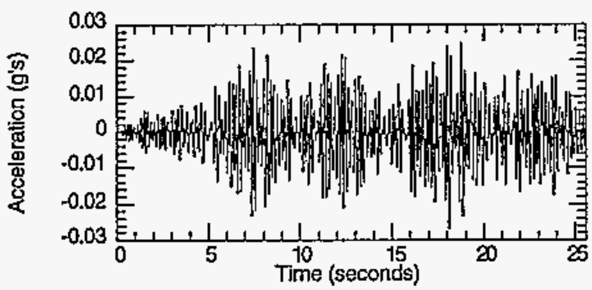

Fig. 8 Typical acceleration time history response at location N-5 for the undamaged bridge.

A forced vibration dynamic analysis was initially done with the bridge in its undamaged state and then repeated for each damaged case A-1 through A-8 and the second undamaged case, Case A-9. Results from these analyses (i.e., monitored acceleration responses) were then analyzed as discussed in the next section.

5. DATA REDUCTION

Results from these analyses (node point accelerations) were then analyzed using similar signal processing techniques as those applied to the refined set of accelerometer data discussed in [4]. Signal processing tasks were performed using MATLAB [12].

Following the time-history analyses, a spectral analysis was conducted using the nine measured responses. The 1024 sample time-history was divided into two 512 sample signal. A Hanning window was applied to each signal and the signals were then fast-Fourier transformed into the frequency domain. The resulting frequency domain signal are then averaged and used to compute power spectral densities (PSD) and the cross power spectrum (CPS). Processing the response signals in this manner simulates the signal processing approach that would be employed to compute modal properties from ambient vibration data.

Sampling parameters were specified that calculated the CPS from 25.6 second time windows discretized with 1024 samples. These parameters yield a resolution of 0.0391 Hz over a frequency range of 0 - 20 Hz. Complex mode shapes are determined from the magnitude and phase of the cross power spectra between the nine channels, N-1 through N-9, relative to the reference response N-3 (see Fig. 7. The amplitude of a mode shape is governed by the magnitude of the cross power spectral density at the mode's associated resonant frequency. Note that the modal amplitude for a particular mode at the reference location N-3 is obtained from its power spectral density. Figure 9 shows a typical cross power spectrum magnitude between channel N-5 relative to channel N-3. The resonant frequencies and mode shape data (first three modes) obtained from this data reduction method, corresponding to the different damage cases, are tabulated in [10].

6. RESULTS

Prior to analyzing the modal data with the various damage identification routines, the mode shape data were first normalized assuming an identity mass matrix as discussed in [4]. Cubic polynomial interpolation procedures discussed in [4] were again employed to obtain modal amplitudes at locations intermediate to the nodes whose response was monitored. Figures 10 through 14 show the results of applying the various damage identification methods to damage case A-6 where two damage locations were specified in the numerical model. The correct damage locations for case A-6 are nodes 40 and 100. All the methods give indications of damage at these locations, however, the damage index method does not yield a value greater than 2 (the criteria for damage) at node 40. Table III summarize the results obtained when the various damage identification methods are applied to the sets of data corresponding to each damage case. Of concern is the fact that the damage index method was the only one that did not give a false positive reading when case A-9 was examined.

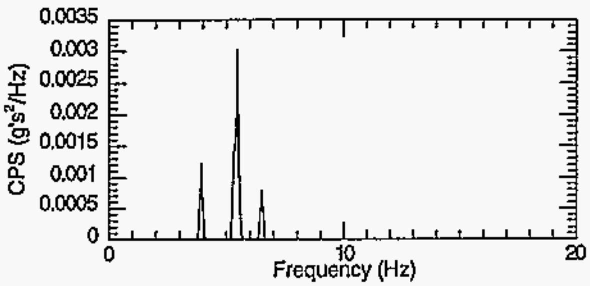

F

ig. 9 Undamaged CPS between channels N-5 and N-3 .

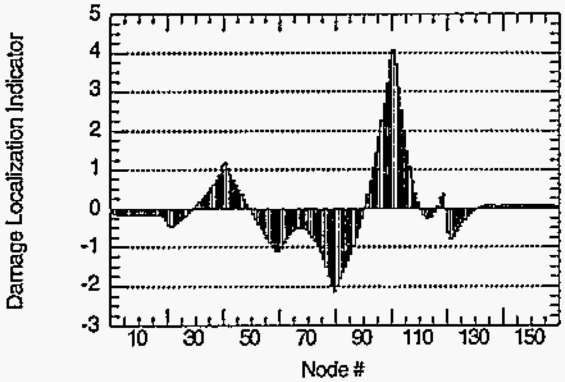

Fig. 10 Damage index method applied to case A-6

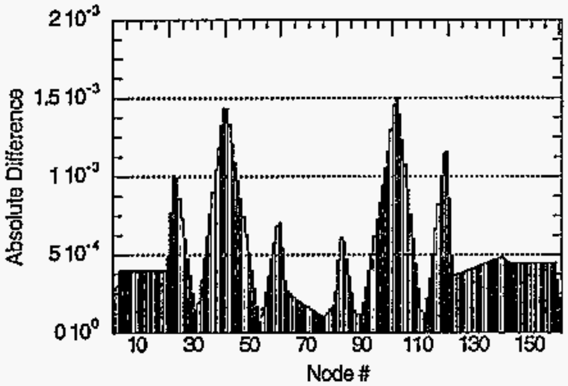

Fig. 11 Change in mode curvature method applied to A-6

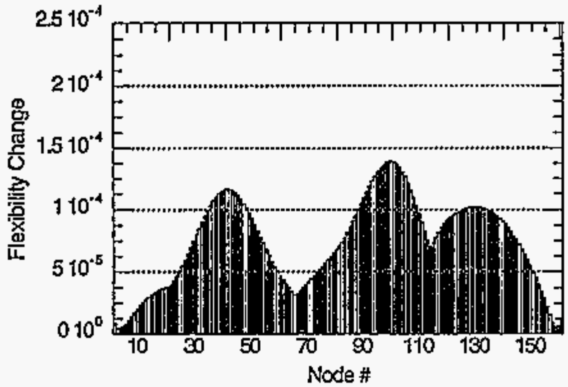

Fig. 12 Change in flexibility method applied to case A-6.

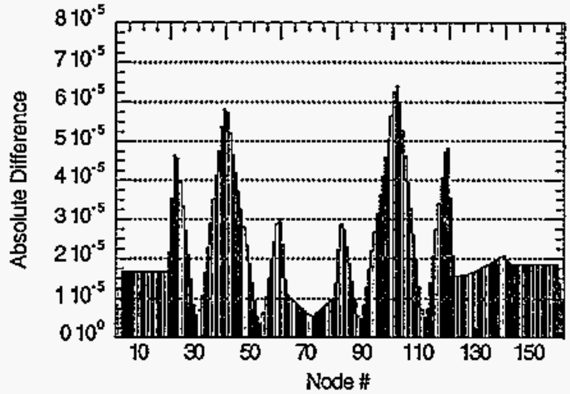

Fig. 13 Change uniform flexibility curvature method applied to case A-6.

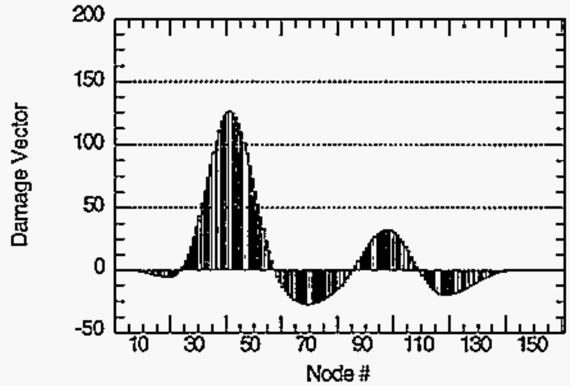

Fig. 14 Change in stiffness method applied to case A-6.

TABLE III

Summary of Damage Detection Results Using Numerical Modal Data

Damage Case	Damage Index Method	Mode Shape Curvature Method	Change in Flexibility Method	Change in uniform Flexibility curvature Method	Change in Stiffness Method
A-1:	●●	○	○	○	○
A-2:	●●	○	○	○	○
A-3:	●	●	○	●	○
A-4: t	●	●	●	●	●
A-5:	●	●	●	●	●
A-6:	●	●	●	●	●
A-7:	○	●	○	○	○
A-8:	●●	●	○	●	○
A-9		F+	F+	F+	F+

● Damage located
●● Damage narrowed down to two locations
●●● Damage narrowed down to three locations
○ Damage not located
F+ Denotes false-positive reading

7. SUMMARY

After benchmarking a finite element model against measured modal data from a bridge in its undamaged and damaged condition, extensive sets of numerical analyses were run with various damage cases simulated in the models. Nodal point acceleration from these runs, at locations corresponding to assumed accelerometer locations, were then processed to yield mode shape and resonant frequency data. It is the authors' opinion that if automated damage identification methods are to become an accepted part of a comprehensive bridge management system, these methods will have to monitor the response of the bridge to ambient (typically traffic induced) vibration. To this end, the data reduction methods used in this study have assumed that the measured input is not monitored.

Five damage identification algorithms were applied to the numerically generated modal data from simulations of the undamaged and damaged bridge. All the algorithms require undamaged and damaged mode shape data . In addition, some of the methods require undamaged and damaged resonant frequencies as well as unit-mass-normalized mode shapes. Using an assumed identity mass matrix to normalize the modes did not adversly effect these methods.

In general, all methods identified damage correctly when damage cases corresponding a cut completely through the bottom flange were examined. However, for several of these methods, if they had been applied blindly, it would be difficult to tell if damage had not occurred at locations other than the actual one. The methods were inconsistent when they were applied to the less severe damage cases. Results of this study show that the damage index method performed the best when the entire set of analyses are considered. This performance is attributed to the methods of normalizing changes in the parameters that are used to indicate damage, that is, curvature of the mode shape. Also, this method is the only one that specifies criteria to quantify when changes in the monitored parameters are indicative of damage. Such a criteria is essential when trying to determine if damage has occurred at more than one location and for preventing false-positive readings.

Although not analytically verified, it is assumed that the false positive readings could possibly be eliminated by taking more average of the data used to obtain the cross-power spectra and, in turn, the mode shape amplitudes. Finally, the authors acknowledge that there are other damage identification method available as well as improvements to the ones used in this study that may offer enhanced capabilities to detect damage from changes in measured modal properties. This study does provide a set of data with which to compare these other methods.

8. ACKNOWLEDGMENTS

Funding for this research was provided to New Mexico State University by the Federal Highway Administration. NMSU, in turn, contacted Los Alamos National Laboratory to perform the analyses reported herein.

9. REFERENCES

1. Farrar, C. R., et al., (1994) "Dynamic Characterization and Damage Detection in the I-40 Bridge over the Rio Grande," Los Alamos National Lab report LA-12767-MS.

2. Farrar, C. R. and K. M. Cone (1995) "Vibration Testing of the I-40 Bridge Before and After the Introduction of Damage," Proceedings 13th International Modal Analysis Conference, Nashville, TN.

3. Farrar, C. R., et al., (1995) "Finite Element Analysis of the I-40 Bridge over the Rio Grande," Los Alamos National Lab report LA-12979-MS.

4. Jauregui, D. V. and C. R. Farrar (1996) "Comparison of Damage Identification Algorithms on Experimental Modal Data from a Bridge," Proceedings 14th International Modal Analysis Conference, Dearborn, MI.

5. Stubbs, N., J.-T. Kim, and C. R. Farrar (1995), *Field Verification of a Nondestructive Damage Localization and Severity Estimation Algorithm*, Proceedings 13th International Modal Analysis Conference, Nashville, TN.

6. Pandey, A. K., M. Biswas, and M. M. Samman (1991) "Damage Detection from Changes in Curvature Mode Shapes," *J. of Sound and Vibration*, 145(2), 321-332.

7. Pandey, A. K. and M. Biswas (1994) "Damage Detection from Changes in Flexibility," *J. of Sound and Vibration*, 169(1), 3-17.

8. Zhang, Z., and A. E. Aktan (1995) "The Damage Indices for the Constructed Facilities," *Proceedings of the 13th International Modal Analysis Conf.*, 2, 1520-1529.

9. Zimmerman, D. C. and M. Kaouk (1994) "Structural Damage Detection using a Minimum Rank Update Theory", *J.of Vibration and Acoustics*, **116**, 222-231.

10. Farrar, C. R. and D. V. Jauregui (1995) "Damage Detection Algorithms Applied to Experimental and Analytical Modal Data from the I-40 Bridge," Los Alamos National Lab report (in print).

11. Doebling, S. W., et al., (1995) "Damage Identification in Structures and Mechanical Systems Based on Changes in their Vibration Characteristics: A Detailed Literature Review," Los Alamos National Laboratory report (in preparation).

12.The MathWorks, Inc. (1992) *MATLAB User's Guide*, Natick, MA.